ADVANCED OPTICAL MATERIALS
www.advopticalmat.de

Materials Views
www.MaterialsViews.com

Three Colors Emission from S,N Co-doped Graphene Quantum Dots for Visible Light H_2 Production and Bioimaging

Dan Qu, Zaicheng Sun, Min Zheng, Jing Li, Yongqiang Zhang, Guoqiang Zhang, Haifeng Zhao, Xingyuan Liu, and Zhigang Xie*

A facile solvothermal route to synthesize S,N co-doped graphene quantum dots (S,N-GQDs) with unique optical properties is demonstrated. Three absorption bands are observed at 338, 467, and 557 nm, which is different from any previous reports. The photoluminescent spectra display emissions in three primary colors that are independent of the excitation wavelength, within the excitation wavelength ranges of 340–420 nm, 460–540 nm, and 560–620 nm. The PL excitation spectra indicate that each emission is related to a single excitation band. It is proposed that three independent luminescent centers coexist in S,N-GQDs because the doping with S and N may change the chemical environment of the GQDs. However, energy-transfer processes usually do not occur among the independent luminescent centers under different wavelength light excitation. Heteroatom-doping of GQDs provides an attractive means of effectively tuning their optical properties for the purpose of exploiting new applications in visible-light photocatalytic and bioimaging. S,N-GQDs/TiO_2 composites exhibit better hydrogen production activities under visible light ($\lambda > 420$ nm) than commercial TiO_2 (P25), owing to the presence of characteristic absorption bands in the visible region. Furthermore, the S,N-GQDs have a pronounced biocompatibility and bioimaging ability under long-wavelengths excitation for live A549 cells.

1. Introduction

Graphene quantum dots (GQDs) have emerged and initiated tremendous research interest as nascent quantum dots (QDs), which are graphene nanosheets of less than 100 nm in size.[1] They have the potential to replace traditional, toxic, metal-based semiconductor QDs currently in use, owing to their outstanding optical properties, low-toxicity, good biocompatibility, and robust chemical inertness,[2] which leads to various applications in bioimaging,[3] photocatalysis,[4] ion detection,[5] lasing,[6] light-emitting diodes,[7] and photovoltaic devices.[8] Although GQDs exhibit unique properties and functions, there are numerous challenges associated with them, partly due to the lack of emission under long wavelength excitation and broad absorption in the visible region ($\lambda > 400$ nm), therefore controlling the properties of the GQDs is paramount for applications in bioimaging and photocatalysis.

Most recently, doping GQDs with heteroatoms has provided an attractive means of effectively changing the electronic density and tuning their intrinsic properties.[9] It has been demonstrated that carbon materials doped with heteroatoms, having either a larger (N, S) or smaller (P, B) diameter than carbon, show pronounced activities.[10] What is especially worth mentioning is that doping the carbon framework with S induces new properties in carbon-based materials. Up to now, various S-doped carbon-based materials have been reported such as microporous carbon,[11,12] carbon microspheres,[13] activated carbons,[14] graphenes,[15] and co-doped graphenes.[16] Up to now little work has been done to characterize the optical properties that are directly associated with the absorption bands of S,N-GQDs.[12,17] Most reported S,N-GQDs show absorption in the UV region and blue emission under UV excitation. Although we have reported S,N-GQDs with red emission, absorption in the visible region, and PL emission in the long-wavelength region, their emission is not strong enough for bioimaging and photocatalytic applications. Hence, it is highly desirable to understand the optical properties and band structures of S,N-GQDs and their potential applications.

In line with the intensive research on GQDs, S,N-doped carbon nanomaterials, and S-doped carbon nanomaterials, we report here a facile solvothermal synthetic route to develop

D. Qu, Prof. Z. Sun, Dr. M. Zheng, Y. Zhang, G. Zhang, H. Zhao, Prof. X. Liu
State Key Laboratory of Luminescence and Applications
Changchun Institute of Optics
Fine Mechanics and Physics
Chinese Academy of Sciences
3888 East Nanhu Road, Changchun, Jilin 130033, P.R. China
E-mail: sunzc@ciomp.ac.cn
Dr. J. Li, Prof. Z. Xie
State Key Laboratory of Polymer Physics and Chemistry
Changchun Institute of Applied Chemistry
Chinese Academy of Sciences
Changchun 130022, P.R. China
D. Qu, Y. Zhang, G. Zhang
University of Chinese Academy of Sciences
Beijing 100000, P.R. China

DOI: 10.1002/adom.201400549

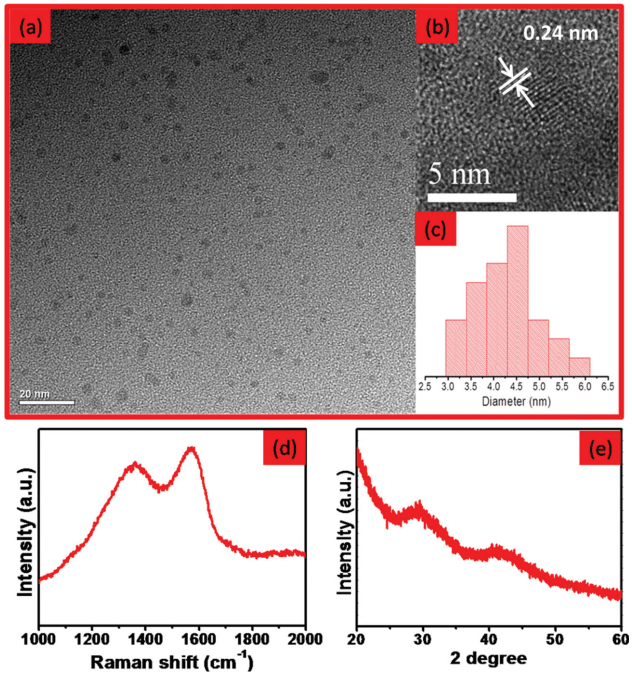

Figure 1. a–c) Transmission electron microscopy (TEM) image (a), high-resolution (HR) TEM image (b), and nanoparticles diameter histogram (c) of as-prepared S,N-GQDs. d,e) Raman spectrum (λ_{ex} = 325 nm) (d) and X-ray diffraction (XRD) pattern (e) of S,N-GQDs.

S,N-GQDs using citric acid (CA) as the carbon source, and thiourea as the N and S source. Dimethylformamide (DMF), as a solvent, may also act as a reactant to further functionalize and passivate the S,N-GQDs, resulting in a high N percentage in the as-prepared S,N-GQDs. In comparison with previously reported GQDs, the as-obtained S,N-GQDs emit three primary colors independently at three excitation wavelengths, namely luminescence at 440, 550, and 650 nm under excitations of 340–420 nm, 460–540 nm, and 560–620 nm, respectively. Each photoluminescence excitation (PLE) spectrum (for the emission at 440, 550, or 650 nm) is related to one single excitation band, which indicates the existence of multiple luminescent centers in the S,N-GQDs. This novel material also shows new UV-vis absorption bands (338, 467, and 557 nm) extending into the visible region induced by the doping with S and N. One of the most notable characteristics is that S,N-GQD/TiO_2 composites prepared from our S,N-GQDs show a remarkable hydrogen production activity under visible light (λ > 420nm) compared to that of pure TiO_2 (P25), implying the considerable potential for applications in environmental protection and energy conversion. Moreover, the S,N-GQDs show a good performance for in-vitro bioimaging.

2. Results and Discussion

2.1. Characterization of S,N-GQDs

Transmission electron microscopy (TEM) images of S,N-GQDs, as shown in **Figure 1**a, reveal that the S,N-GQDs have a uniform dispersion without apparent aggregation. From the high-resolution (HR)TEM images in Figure 1b a clear lattice fringe of 0.24 nm can be seen, which is similar to that of the (1120) facet of graphite,[12] disclosing that the S,N-GQDs have a graphite nature. Figure 1c shows that the as-prepared GQDs are well dispersed with a narrow size distribution with a mean diameter of 4.52 ± 0.62 nm. The corresponding atomic force microscopy (AFM) image reveals a typical topographic height of around 1 nm (Figure S1, Supporting Information), suggesting that most of the as-prepared S,N-GQDs consist of 1 to 3 graphene layers.[15] The above results suggest that the nanoparticles might be composed of nanocrystalline cores of graphitic sp^2 carbon atoms.[18,19] The Raman spectra (λ_{ex} = 325 nm) of the S,N-GQDs is shown in Figure 1d. The as-prepared S,N-GQDs reveal two prominent peaks at 1348 and 1570 cm^{-1}, corresponding to the documented D and G bands, respectively. The intensity ratio of the D and G band (I_D/I_G) is a measurement of the disorder extent, as well as the ratio of sp^3/sp^2 carbons. In our case, the I_D/I_G ratios of the S,N-GQDs is around 0.94, which is close to that of graphene, indicating that relatively high-quality GQDs are produced.[20] The X-ray diffraction (XRD) pattern of the S,N-GQDs is shown in Figure 1e. The spectrum of the S,N-GQDs shows one prominent peak at 26.2° that corresponds to the (002) planes of graphite.[21] To sum it all up, the above results indicate that the as-prepared S,N-GQDs are highly crystalline and graphitic materials.

Prior to gaining further insight into the PL properties of the S,N-GQDs, a series of X-ray photoelectron spectroscopy (XPS) analyses was carried out to determine the composition of the as-produced S,N-GQDs. The XPS full survey spectrum of the S,N-GQDs, as shown in **Figure 2**a, presents 5 peaks at 164, 227, 284, 400, and 533 eV, which correspond to S 1s, S 2p, C 1s, N 1s and O 1s, respectively. This indicates that the GQDs prepared from thiourea are doped with N and S. The high-resolution C 1s XPS spectrum (Figure 2b) shows 3 predominant graphitic peaks at 284.4, 285.5, and 286.8 eV, corresponding to sp^2 C in graphene (C–C), sp^3 C in C–N, C–S, and C–O and C=O, respectively.[22] However, no peak at 288.4 eV is observed, which indicates that no –COOH group exist in the S,N-GQDs.[12,23,24] The high-resolution N 1s spectrum of the S,N-GQDs (Figure 2c) shows two pronounced peaks at 399.4 and 401.4 eV, which can be attributed to the pyrrolic N(C–N–C) and graphitic N or N–H bands, respectively.[19,24] Compared to S,N co-doped GQDs that have been prepared in water,[12] our S,N-GQDs prepared in DMF exhibit a higher percentage of N in the full XPS spectra and higher percentage of pyrrolic N. This may be attributed to the use of DMF, as DMF may react with the functional groups of the GQDs to form tertiary N, which has a similar binding energy to pyrrolic N. The O 1s spectrum (Figure 2d) shows two peaks at 531.0 and 532.1 eV, which can be attributed to C=O and C–OH/C–O–C groups, respectively.[25] Moreover, the high-resolution spectrum of S 2p XPS (Figure 2e) of S,N-GQDs clearly shows two peaks at 162.7 and 168.1 eV, which represent S $2p^{3/2}$ of thiophene and S=O.[17] Furthermore, Figure 2f shows the elemental analysis results of the S,N-GQDs, confirming that the C content is 62.8%, which illustrates that the S,N-GQDs is mainly based on carbon. The N and S contents were 14.3% and 9.6%, respectively, which further verifies that the GQDs are heavily doped with S and N. Thus, the thiourea molecules play a dual role in the

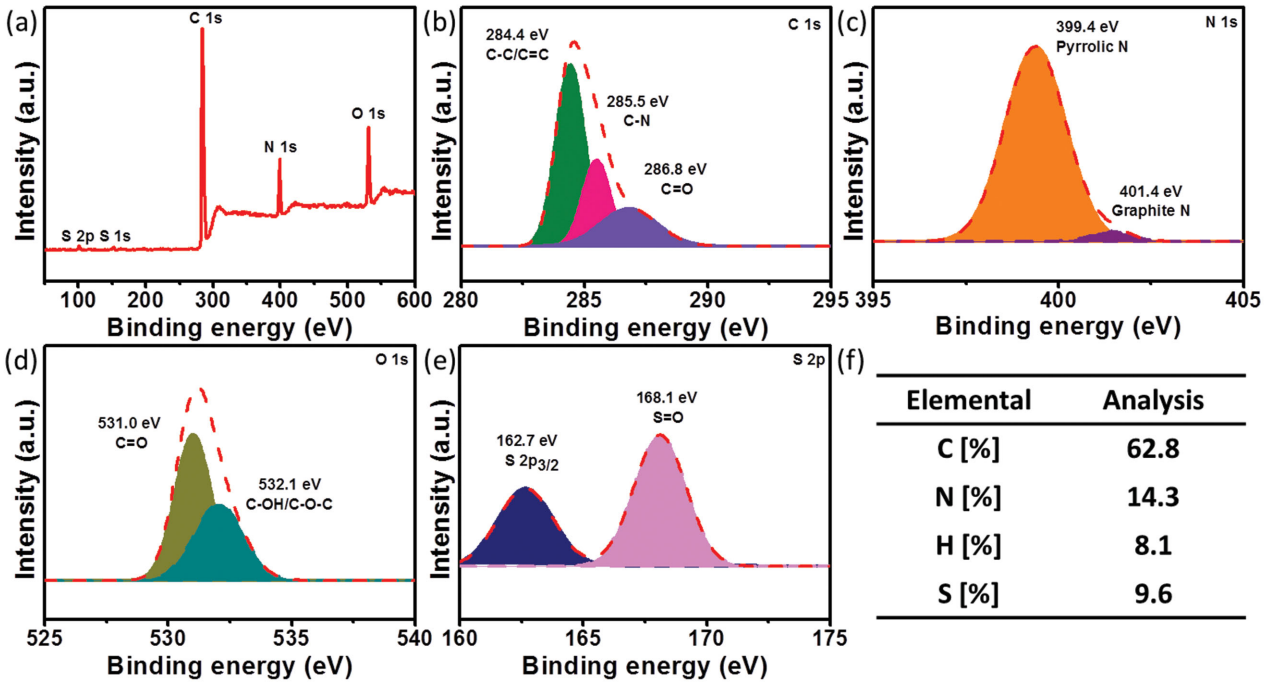

Figure 2. a–e) XPS full survey (a), high-resolution XPS of C 1s (b), N 1s (c), O 1s (d) and S 2p (e) spectra of S,N-GQDs. f) Elemental analysis results of S,N-GQDs.

solvothermal process, one role is its use as the S and N dopant source, the other is acting as the passivation agent to form the edge functional groups, both of which roles greatly contribute to the PL enhancement of the GQDs.[26] All the above results demonstrate that the as-prepared GQDs are co-doped with S and N. In addition, Fourier-transform infrared (FTIR) spectra (Figure S2, Supporting Information) of the S,N-GQDs showed the following characteristic peaks: stretching vibrations of C–H at 2923 cm^{-1}, asymmetric stretching vibrations of C=S and C–S at 1185 cm^{-1}, and 782 cm^{-1}, respectively, bending vibrations of N-H at 1558 cm^{-1}, and the vibrational peak of C=O at 1650 cm^{-1},[27] which is consistent with the corresponding XPS results. All of the above results indicate that the as-prepared GQDs are S,N co-doped GQDs.

2.2. Optical Properties of S,N-GQDs

The UV-vis spectrum of our S,N-GQDs, as shown in **Figure 3**a, displays absorption bands centered at 338, 467, and 557 nm, which are similar to those of GQDs prepared by a hydrothermal graphene oxide reduction method.[28] The origin of these peaks is related to electron transition in heteroatom-containing GQDs. The absorption peak at 338 nm is due to the n→π^* transition of the conjugated C=O and C=N bonds.[24] The absorption peak at 467 nm corresponds to the n→π^* transition of the conjugated C=N and C=S bonds,[12,29] and the absorption peak at 557 nm is attributed to the n→π^* transition of the conjugated C=S bond.[12] The dependence of the emission wavelengths and intensity on the excitation wavelength is a common phenomenon observed in carbon-based fluorescent materials. However, there are some significant differences in the optical properties between the as-obtained S,N-GQDs and traditional GQDs.

In the PL spectra (Figure 3b,d,f and Figure S3 in the Supporting Information) the as-prepared S,N-GQDs exhibit three excitation-wavelength-independent photoluminescence (PL) regions with emission peaks at 440 (blue), 550 (green), and 640 nm (red) at excitation wavelength intervals ranging from 340 to 420 nm, 460 to 540 nm, and 560 to 620 nm, respectively. This indicates that each emission is related to a unified chromophore on the S,N-GQDs. Moreover, the chromophore group emits light at a specific wavelength under a specific range of excitation light. When the excitation light nears the transition wavelength, the PL spectra show 2 emission bands, indicating that 2 kinds of chromophores were excited by the light. The PL excitation (PLE) spectra of S,N-GQDs are shown in Figure 3c and Figure S4 in the Supporting Information. It shows that the blue (λ_{em} = 440), green (λ_{em} = 540), and red (λ_{em} = 640) emission originates from the excitation bands located at 370, 450, and 480 nm, respectively. It should be noted that each emission was excited by a single excitation band. This is contrary to previous reports where multiple PLE bands contribute to one emission, which means cross-band interactions exist in the S-doped GQDs.[30] Figure S5 in the Supporting Information shows the PL spectra of two kinds of N-doped GQDs emitting blue and green light under UV and visible light excitation, respectively. Only green light is emitted under UV and visible light excitation when these two N-GQDs are physically mixed together. We therefore deduce that three kinds of chromophores must co-exist in our S,N-GQDs and there can be no energy transfer between them. The wavelengths of the PLE peaks correspond well with those of the UV–vis absorption. When light with a

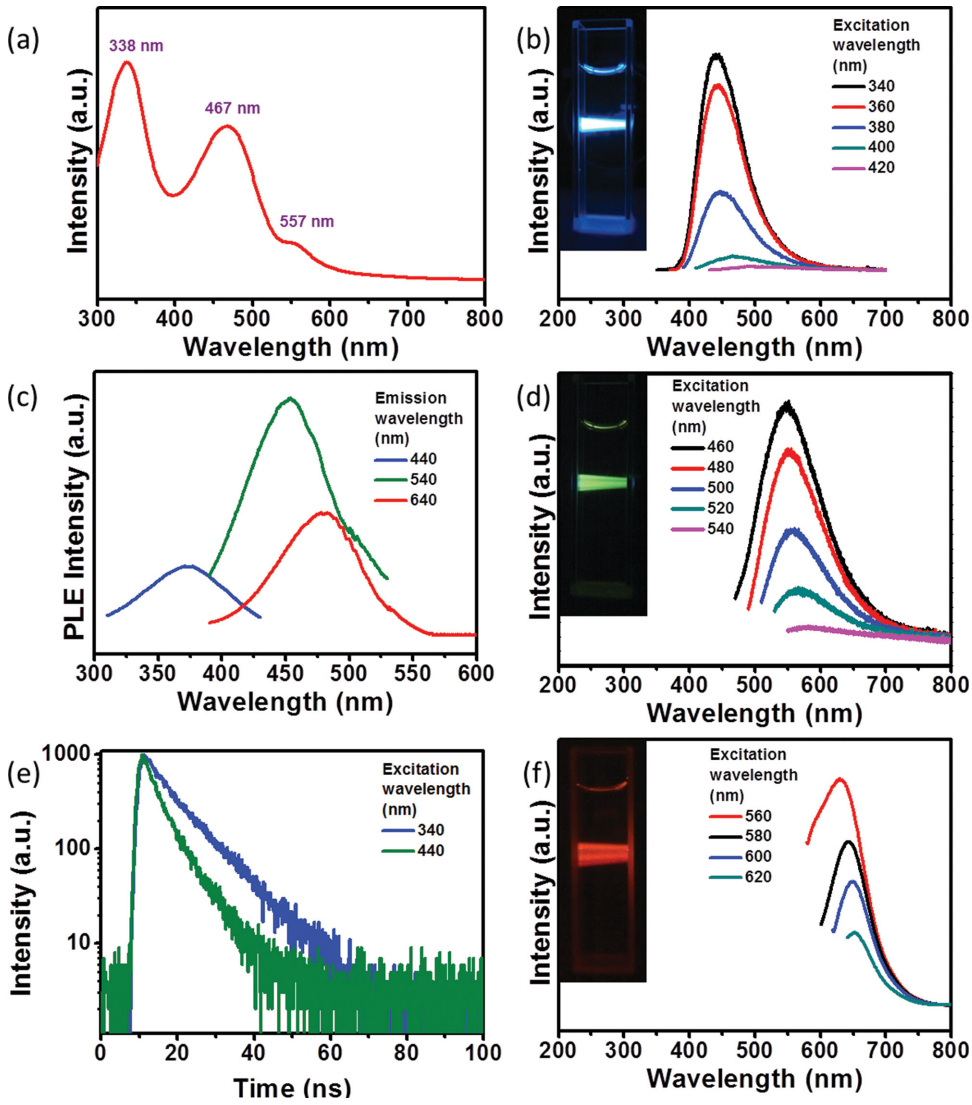

Figure 3. a) UV–vis absorption and b,d,f) photoluminescent (PL) spectra of S,N-GQDs under different excitation wavelengths in the range of 340–420 nm (b), 460–540 nm (d), and 560–620 nm (f) (excitation wavelength interval 20 nm). The insets in (b,d,f) are optical images of the S,N-GQDs aqueous solution excited at 340, 460, and 560 nm, respectively. c) The PLE spectra of S,N-GQDs for the emission at 440, 540, and 650 nm. e) PL decay time of S,N-GQDs under different excitation wavelengths of 340 and 460 nm.

wavelength of 340 nm is absorbed by the chromophore containing a C=O group, the excited n→π^* transition of the C=O emits blue emission (440 nm). Long-wavelength light cannot be absorbed by a C=O chromophore, however, it can be absorbed by the chromophores containing a C=N or C=S group, which results in green or red emission. The PL quantum yields of the S,N-GQDs were 61%, 45%, and 8% for the emissions at 340, 440, and 540 nm, which represent the blue, green, and red emissions, respectively. The PL decay of S,N-GQDs could be fitted by a double exponential function (Figure 3e). The average lifetimes of the S,N-GQDs emission were 10 and 6 ns for excitations at 340 and 440 nm, respectively (Table S1, Supporting Information).

On the basis of the above results and previous results on N-doped GQDs,[24,31] a model for the PL mechanism (**Scheme 1**) is proposed to explain the PL process of S,N-GQDs. It is clear that there are O, N, and S states, which may be related to the π^* orbital of the C=O, C=N, and C=S bonds in the S,N-GQDs. If the excitation energy is above 3.10 eV, the chromophore containing C=O bonds is excited and blue light is emitted from the S,N-GQDs. If N is introduced into conjugated molecules, the n→π^* transition of C=N results in a red-shift of the absorption and emission band.[4] Therefore, if the excitation light energy is about 2.75 eV the light was absorbed by the chromophore containing the C=N group and green light was emitted. We also observed cyan light, a mixture of blue and green, that was emitted from our S,N-GQDs under an excitation wavelength of 440 nm. The N and O state overlap in some degree. Furthermore, S doping induces the insertion of the S π^* orbital between the N π^* and the C n orbital and forms an S state due to the low electronegativity of S.[9] It can thus absorb light with a lower energy and emit light with a longer wavelength.

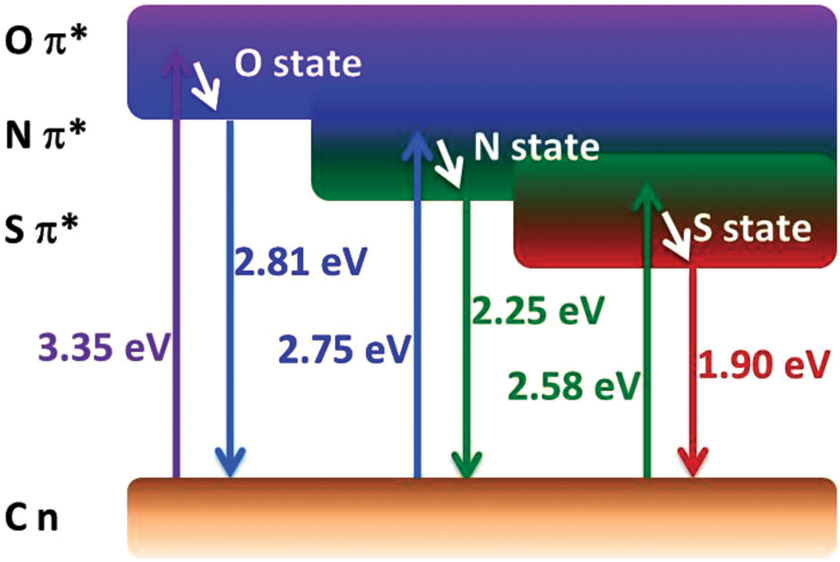

Scheme 1. The proposed energy-level diagram of the S,N-GQDs.

2.3. Photocatalytic H_2 Production

As these small S,N-GQDs show a broad absorption in the visible-light region, they could be employed as a powerful energy harvester for photocatalysts in environmental and energy issues. TiO_2 is a currently used top of the range photocatalyst that offers a facile route for environmental therapy and energy crises.[32,33] However, a crucial issue to its practical applications lies in its wide bandgap, which results in the downside that only UV light, which encompasses less than 5% of natural sunlight, can be absorbed.[32] In view of the broad visible-light absorption band of our S,N-GQDs, we expected that combining S,N-GQDs with TiO_2 in a composite system for photocatalysis would realize the efficient usage of the full solar spectrum. We prepared the S,N-GQDs/TiO_2 composites by simply stirring P25 TiO_2 nanocrystals in an S,N-GQDs aqueous solution over 24 hours. **Figure 4**a shows the TEM images of the as-prepared photocatalyst S,N-GQDs/TiO_2. It clearly displays that the S,N-GQDs are anchored on the TiO_2 surface. The insets show the corresponding HRTEM images and fast Fourier-transform (FFT) spot diagrams of TiO_2 and S,N-GQDs with defined lattice fringes, indicating that the S,N-GQDs are attached to the surface of the TiO_2 nanoparticles. Figure 4b shows the photocatalytic performance of our S,N-GQDs/TiO_2 loaded with 1.0 wt% Pt under visible light ($\lambda > 420$ nm) illumination for H_2 production. For pure TiO_2 nanoparticles, no H_2 production is detected under visible light.[34] As shown in Figure 4b,c, when a trace amount (0.71 wt%) of S,N-GQDs was loaded onto the surface of the TiO_2 nanoparticles, around 2.62 mol of H_2 was produced per hour for 50 mg of photocatalyst. The H_2 production rate reached its maximum of 4.3 mol/hour for 50 mg TiO_2 nanoparticles loaded with 1.24 wt% S,N-GQDs under

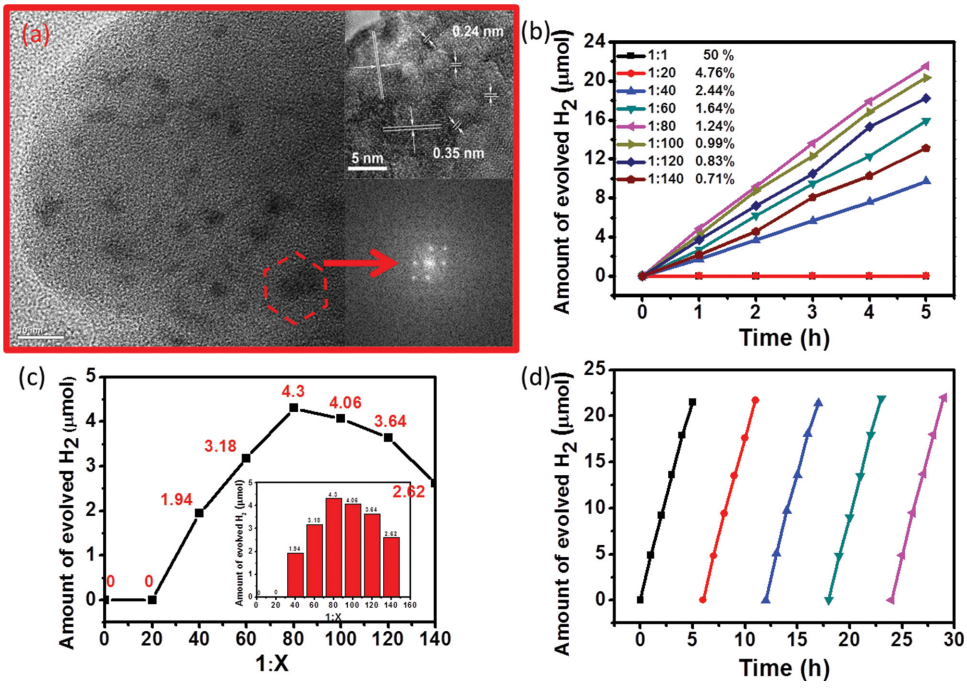

Figure 4. a) TEM images of S,N-GQDs/TiO_2 composites (the insets show the HRTEM and FFT images), b) the amount of evolved H_2 from 50 mg of P25 TiO_2 nanoparticles loaded with different amounts of as-prepared S,N-GQDs, c) the average amount of evolved H_2 per hour from 50 mg of TiO_2 nanoparticles loaded with different amounts of as-prepared S,N-GQDs, d) 5 repeat cycle experiments of 50 mg of P25 TiO_2 nanoparticles loaded with 1.24 wt% S,N-GQDs.

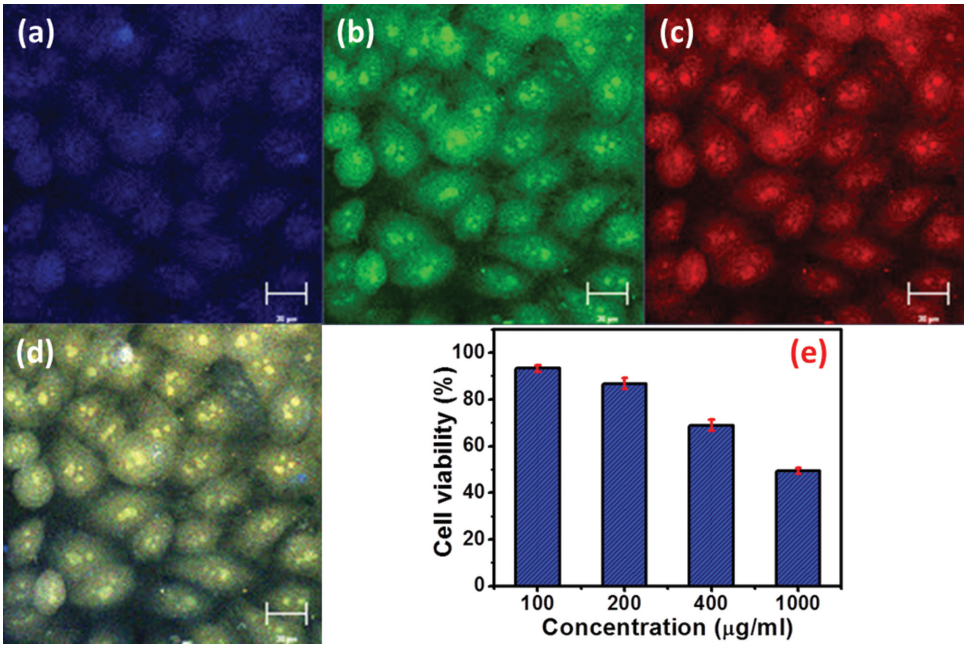

Figure 5. a–c) Confocal fluorescence images of A549 cells incubated with S,N-GQDs for 1 hour imaged under 405 nm (a), 488 nm (b), and 555 nm (c) excitation. d) Overlay image of (a–c). The scale bars correspond to 20 μm. e) Cell viability of A549 after incubation with S,N-GQDs for 48 h, determined by MTT assay.

visible light. The S,N-GQDs/TiO_2 composite photocatalyst displayed an excellent stability. The H_2 production rate was constant for 5 repeat cycles (Figure 4d).

2.4. Bioimaging Applications of S,N-GQDs

Our S,N-GQDs display a strong PL emission at 450, 550, and 630 nm under excitation light of 350, 460, and 560 nm, respectively. These features make our S,N-GQDs excellent probes for bioimaging, which is demonstrated by imaging live A549 cells. As shown in **Figure 5**a–d after incubation with S,N-GQDs the cells displayed blue, green, and red colors under excitation at 405, 488, and 555 nm, respectively. The viability of the A549 cells was examined after the cells had been exposed to 0–1000 μg mL^{-1} of S,N-GQDs, and the cytotoxicity of S,N-GQDs was investigated using a standard 3-(4,5-dimethylthiazol-2-yl)-2,5-diphenyltetrazolium bromide (MTT) assay (Figure 5e). A 93% viability could be observed after incubating the A549 cells with S,N-GQDs (100 g mL^{-1}) for 48 h. The cell viability remained at 70% even if the concentration of S,N-GQDs was increased to 400 g mL^{-1}. These results indicate that S,N-GQDs can potentially be used in bioimaging.

3. Conclusions

S,N-GQDs were prepared via a solvothermal route from CA and thiourea. The doped heteroatoms (S,N) rendered unique optical properties to the S,N-GQDs. The S,N-GQDs showed two absorption bands at 467 and 557 nm in the visible-light region. The PL emission could be tuned from blue, green to red under UV and visible light excitation. Our GQDs mainly displayed three emission peaks that were independent of the excitation wavelength at 440, 550, and 650 nm under excitation wavelengths ranging from 340 to 420 nm, 460 to 540 nm, and 560 to 620 nm, respectively. PLE investigation indicated that these three emissions are related to three kinds of chromophores in the S,N-GQDs, which may be attributed to the conjugation of the C=O, C=N, and C=S groups with the graphene core. Because of the wide absorption range in the visible region our S,N-GQDs could be used as a sensitizer for photocatalytic reactions. H_2 production from water splitting was demonstrated by loading S,N-GQDs on TiO_2 nanocrystals. They clearly showed H_2 production (rate is ca. 4.3 mol/hour) under visible-light irradiation. On the other hand our S,N-GQDs also showed strong emission under visible-light excitation, therefore, we were also able to demonstrate that our S,N-GQDs could be employed as a good bioimaging agent.

4. Experimental Section

Materials: All chemicals were commercially available, of analytical grade and were used without any further purification. Citric acid (CA), thiourea, and DMF were purchased from Aladdin Reagent Company or Beijing Chemical Reagent Company.

Synthesis of S,N co-Doped GQDs (S,N-GQDs): 0.19 g (1 mmol) CA and 0.23 g (3 mmol) thiourea were dissolved into 4 mL DMF and stirred to form a clear solution. Then the solution was transferred into a 20 mL Teflon-lined stainless steel autoclave. The sealed autoclave was heated to 180 °C in an electric oven and kept there for an additional 8 h. The final product was collected by adding ethanol into the solution and then centrifuged at 9000 rpm for 15 min. The solid could be easily redispersed into water.

Photocatalytic Activity Measurements: Preparation of S,N-GQDs/TiO_2 composites: 50 mg of P25 TiO_2 was dispersed into the GQD aqueous solution and kept stirring for 24 h. Then the S,N-GQDs/TiO_2 composites

were collected by centrifugation at 8500 rpm for 30 min. The solid was dried at 70 °C for 24 h.

Photocatalytic Hydrogen Generation: 50 mg of photocatalyst loaded with 1.0 wt% of Pt was placed into an aqueous methanol solution (120 mL, 25%) in a closed gas-circulation system (Perfect Light Company Labsolar-III (AG)). The UV-light and visible-light irradiations were obtained from a 300 W Xe lamp (Perfect Light Company Solaredge 700) without and with a UVCUT-420 nm filter (Newport), respectively. Methanol was used as a sacrificial reagent. The amount of generated H_2 was determined with an online gas chromatograph (Shimadzu GC-2014c).

Biocompatibility Testing: A549 cells harvested in a logarithmic growth phase were seeded in 96-well plates at a density of 105 cells/well and incubated in Dulbecco's modified Eagle's medium (DMEM) for 24 h. The medium was then replaced by S,N-GQDs, at a final equivalent concentration from 0.16 to 1000 μg mL^{-1}. The incubation was continued for 48 h. Then, 20 μL of MTT solution in phosphate-buffered saline (PBS) with a concentration of 5 mg mL^{-1} was added and the plates were incubated for another 4 h at 37 °C, followed by removal of the culture medium containing MTT and addition of 150 μL of dimethylsulfoxide (DMSO) to each well to dissolve the formazan crystals formed. Finally, the plates were shaken for 10 min, and the absorbance of formazan product was measured at 490 nm by a microplate reader.

Confocal Laser Scanning Microscope Studies: The cellular uptake by the A549 cells was examined by confocal laser scanning microscopy (CLSM). A549 cells were seeded in 6-well culture plates at a density of 5×10^4 cells per well and allowed to adhere for 24 h. After that, the cells were treated with S,N-GQDs (2 mg mL^{-1}) for 1 h at 37 °C. After that, the supernatant was carefully removed and the cells were washed three times with PBS. Subsequently, the cells were fixed with 800 μL of 4% formaldehyde in each well for 20 min at room temperature and washed twice with PBS again. The slides were mounted and the cellular localization was observed with a confocal laser scanning microscope (Carl Zeiss LSM 780).

Characterization: Absolute quantum-yield measurements were performed with a calibrated integrating sphere on an Edinburgh FLS 920 spectrometer. Lifetime experiments were obtained on an Edinburgh TSCPS FL 920. UV–vis absorption spectra were conducted on a Shimadzu UV-2450 spectrophotometer. X-ray photoelectron spectra were obtained on a Thermo Scientific ESCALAB 250 Multitechnique surface analysis with an Al Kα X-ray monochromator, pass energy 20 eV. Raman spectra were recorded on a Jobin Yvon Horiba LAB-RAM Infinity using a 325-nm laser beam. Atomic force microscopy (AFM) images were captured on a Multimode 8 (Bruker Co.) in the tapping mode. High-resolution TEM (HRTEM) images and fast Fourier-transform (FFT) spot diagrams were recorded using a FEI-TECNAI G2 transmission electron microscope operating at 200 kV. Fourier-transform infrared (FT-IR) spectra of GQDs were recorded using KBr pellets with a Bruker Vertex 70 spectrometer from 4000–500 cm^{-1}. Fluorescence emission spectra were recorded on a LS-55 fluorophotometer.

Supporting Information

Supporting Information is available from the Wiley Online Library or from the author.

Acknowledgements

The authors thank the National Natural Science Foundation of China (No. 21301166, 21201159, 61306081 and 61176016), and the Science and Technology Department of Jilin Province (No. 20130522127JH, and 20121801) is gratefully acknowledged. Z.S. thanks the support of the "Hundred Talent Program" of CAS and Innovation and Entrepreneurship Program of Jilin. The project was supported by the Open Research Fund of the State Key Laboratory of Polymer Physics and Chemistry.

Received: November 14, 2014
Revised: November 28, 2014
Published online: January 2, 2015

[1] L. A. Ponomarenko, F. Schedin, M. I. Katsnelson, R. Yang, E. W. Hill, K. S. Novoselov, A. K. Geim, *Science* **2008**, *320*, 356.
[2] a) S. N. Baker, G. A. Baker, *Angew. Chem. Int. Ed.* **2010**, *49*, 6726; b) L. Cao, X. Wang, M. J. Meziani, F. Lu, H. Wang, P. G. Luo, Y. Lin, B. A. Harruff, L. M. Veca, D. Murray, S. Y. Xie, Y. P. Sun, *J. Am. Chem. Soc.* **2007**, *129*, 11318.
[3] a) S. Zhu, J. Zhang, C. Qiao, S. Tang, Y. Li, W. Yuan, B. Li, L. Tian, F. Liu, R. Hu, H. Gao, H. Wei, H. Zhang, H. Sun, B. Yang, *Chem. Commun.* **2011**, *47*, 6858; b) A. P. Alivisatos, W. Gu, C. Larabell, *Annu. Rev. Biomed. Eng.* **2005**, *7*, 55; c) X. T. Zheng, A. Than, A. Ananthanaraya, D.-H. Kim, P. Chen, *ACS Nano* **2013**, *7*, 6278; d) M. Zhang, L. Bai, W. Shang, W. Xie, H. Ma, Y. Fu, D. Fang, H. Sun, L. Fan, M. Han, C. Liu, S. Yang, *J .Mater. Chem.* **2012**, *22*, 7461.
[4] H. Li, X. He, Z. Kang, H. Huang, Y. Liu, J. Liu, S. Lian, C. H. A. Tsang, X. Yang, S.-T. Lee, *Angew. Chem. Int. Ed.* **2010**, *49*, 4430.
[5] a) M. Zheng, Z. Xie, D. Qu, D. Li, P. Du, X. Jing, Z. Sun, *ACS Appl. Mater. Interfaces* **2013**, *5*, 13242; b) A. Ananthanarayanan, X. Wang, P. Routh, B. Sana, S. Lim, D.-H. Kim, K.-H. Lim, J. Li, P. Chen, *Adv. Funct. Mater.* **2014**, *24*, 3021; c) J.-M. Bai, L. Zhang, R.-P. Liang, J.-D. Qiu, *Chem. Eur. J.* **2013**, *19*, 3822.
[6] H.-J. Eisler, V. C. Sundar, M. G. Bawendi, M. Walsh, H. I. Smith, V. Klimov, *Appl. Phys. Lett.* **2002**, *80*, 4614.
[7] N. Tessler, V. Medvedev, M. Kazes, S. Kan, U. Banin, *Science* **2002**, *295*, 1506.
[8] V. Gupta, N. Chaudhary, R. Srivastava, G. D. Sharma, R. Bhardwaj, S. Chand, *J. Am. Chem. Soc.* **2011**, *133*, 9960.
[9] S. Yang, J. Sun, X. Li, W. Zhou, Z. Wang, P. He, G. Ding, X. Xie, Z. Kang, M. Jiang, *J. Mater. Chem. A* **2014**, *2*, 8660.
[10] a) R. Liu, D. Wu, X. Feng, K. Muellen, *J. Am. Chem. Soc.* **2011**, *133*, 15221; b) W.-W. Liu, Y.-Q. Feng, X.-B. Yan, J.-T. Chen, Q.-J. Xue, *Adv. Funct. Mater.* **2013**, *23*, 4111; c) Y. Li, Y. Zhao, H. Cheng, Y. Hu, G. Shi, L. Dai, L. Qu, *J. Am. Chem. Soc.* **2011**, *134*, 15.
[11] Y. Xia, Y. Zhu, Y. Tang, *Carbon* **2012**, *50*, 5543.
[12] D. Qu, M. Zheng, P. Du, Y. Zhou, L. Zhang, D. Li, H. Tan, Z. Zhao, Z. Xie, Z. Sun, *Nanoscale* **2013**, *5*, 12272.
[13] M. Zheng, H. Zhang, Y. Xiao, H. Dong, Y. Liu, R. Xu, Y. Hu, B. Deng, B. Lei, X. Liu, *Mater. Lett.* **2013**, *109*, 279.
[14] T. J. Bandosz, J. Matos, M. Seredych, M. S. Z. Islam, R. Alfano, *Appl. Catal. A* **2012**, *445–446*, 159.
[15] Z. Yang, Z. Yao, G. Li, G. Fang, H. Nie, Z. Liu, X. Zhou, X. a. Chen, S. Huang, *ACS Nano* **2011**, *6*, 205.
[16] J. Liang, Y. Jiao, M. Jaroniec, S. Z. Qiao, *Angew. Chem. Int. Ed.* **2012**, *51*, 11496.
[17] Y. Dong, H. Pang, H. B. Yang, C. Guo, J. Shao, Y. Chi, C. M. Li, T. Yu, *Angew. Chem. Int. Ed.* **2013**, *52*, 7800.
[18] Y. P. Sun, B. Zhou, Y. Lin, W. Wang, K. A. S. Fernando, P. Pathak, M. J. Meziani, B. A. Harruff, X. Wang, H. Wang, P. G. Luo, H. Yang, M. E. Kose, B. Chen, L. M. Veca, S. Y. Xie, *J. Am. Chem. Soc.* **2006**, *128*, 7756.
[19] W. Lu, X. Qin, S. Liu, G. Chang, Y. Zhang, Y. Luo, A. M. Asiri, A. O. Al-Youbi, X. Sun, *Anal. Chem.* **2012**, *84*, 5351.
[20] J. Lu, P. S. E. Yeo, C. K. Gan, P. Wu, K. P. Loh, *Nat. Nano* **2011**, *6*, 247.
[21] a) O. Chuhei, N. Ayato, *J. Phys.: Condens. Matter.* **1997**, *9*, 1; b) L. B. Biedermann, M. L. Bolen, M. A. Capano, D. Zemlyanov, R. G. Reifenberger, *Phys. Rev. B* **2009**, *79*, 125–411.
[22] X. Jia, J. Li, E. Wang, *Nanoscale* **2012**, *4*, 5572.
[23] Y. Dong, J. Shao, C. Chen, H. Li, R. Wang, Y. Chi, X. Lin, G. Chen, *Carbon* **2012**, *50*, 4738.
[24] D. Qu, M. Zheng, L. Zhang, H. Zhao, Z. Xie, X. Jing, R. E. Haddad, H. Fan, Z. Sun, *Sci. Rep.* **2014**, *4*, 5294.
[25] H. Ming, Z. Ma, Y. Liu, K. Pan, H. Yu, F. Wang, Z. Kang, *Dalton Trans.* **2012**, *41*, 9526.

[26] S. Qu, X. Wang, Q. Lu, X. Liu, L. Wang, *Angew. Chem. Int. Ed.* **2012**, *51*, 12215.
[27] D. Pan, J. Zhang, Z. Li, C. Wu, X. Yan, M. Wu, *Chem. Commun.* **2010**, *46*, 3681.
[28] D. Pan, J. Zhang, Z. Li, M. Wu, *Adv. Mater.* **2010**, *22*, 734; b) L. Tang, R. Ji, X. Cao, J. Lin, H. Jiang, X. Li, K. S. Teng, C. M. Luk, S. Zeng, J. Hao, S. P. Lau, *ACS Nano* **2012**, *6*, 5102.
[29] E. M. Geniès, A. Boyle, M. Lapkowski, C. Tsintavis, *Synth. Met.* **1990**, *36*, 139.
[30] X. Li, S. P. Lau, L. Tang, R. Ji, P. Yang, *Nanoscale* **2014**, *6*, 5323.
[31] M. A. Sk, A. Ananthanarayanan, L. Huang, K. H. Lim, P. Chen, *J. Mater. Chem. C* **2014**, *2*, 6954.
[32] a) X. Chen, S. S. Mao, *Chem. Rev.* **2007**, *107*, 2891; b) J. Li, W. Ma, C. Chen, J. Zhao, H. Zhu, X. Gao, *J. Mol. Catal. A: Chem.* **2007**, *261*, 131.
[33] a) Z. Kang, C. H. A. Tsang, Z. Zhang, M. Zhang, N.-b. Wong, J. A. Zapien, Y. Shan, S.-T. Lee, *J. Am. Chem. Soc.* **2007**, *129*, 5326; b) Z. Kang, C. H. A. Tsang, N.-B. Wong, Z. Zhang, S.-T. Lee, *J. Am. Chem. Soc.* **2007**, *129*, 12090; c) Z. Kang, Y. Liu, C. H. A. Tsang, D. D. D. Ma, X. Fan, N.-B. Wong, S.-T. Lee, *Adv. Mater.* **2009**, *21*, 661.
[34] G. Xie, K. Zhang, B. Guo, Q. Liu, L. Fang, J. R. Gong, *Adv. Mater.* **2013**, *25*, 3820.